

Sodium Vanadium Oxide $\text{Na}_2\text{V}_6\text{O}_{16}\cdot 3\text{H}_2\text{O}$ Nanorings: A New Room-Temperature Ferromagnetic Semiconductor

Yan Xue,^a Xiaodong Zhang,^a Jiajia Zhang,^a Jian Wu,^a Yongfu Sun,^{a,b} Yangchao Tian,^b and Yi Xie*^a

S1. $(\text{NH}_4)_2\text{V}_6\text{O}_{16}\cdot 5\text{H}_2\text{O}$ nanorings and nanoloops

Synthesis of $(\text{NH}_4)_2\text{V}_6\text{O}_{16}\cdot 5\text{H}_2\text{O}$ nanorings and nanoloops: The synthesis method of $(\text{NH}_4)_2\text{V}_6\text{O}_{16}\cdot 5\text{H}_2\text{O}$ nanorings and microloops was similar as $\text{Na}_2\text{V}_6\text{O}_{16}\cdot 3\text{H}_2\text{O}$ in a hydrothermal process. In a typical process, 2 mmol NH_4VO_3 and 0.5 mmol Na_2CO_3 powders were dissolved into 30 ml distilled water and strongly stirred for several minutes. Then 1 ml 30% hydrogen peroxide (H_2O_2) was added into the above suspension. After gently stirring at room temperature for 1 minute, the all solution was orange V(V) diperoxo aqueous solution with a pH of about 9.0, adjust the pH of the whole solution about 2.0 with 2 M HCl. At last the solution was transferred to a teflon-lined stainless steel autoclave with a capacity of 42 ml, and the autoclave was sealed and maintained at 200 °C for 24 h. The reaction system was then allowed to cool to room temperature. The final product was collected by centrifugation, washed with deionized water and ethanol three times respectively to remove any possible ionic remnants, then dried in vacuum at 50 °C for 5h.

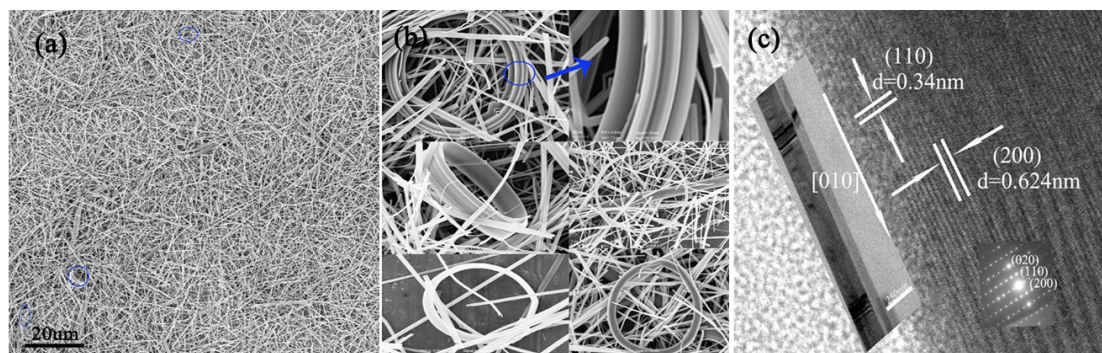


Figure S1. (a, b) Low- and high-magnification FESEM images of the as-prepared $(\text{NH}_4)_2\text{V}_6\text{O}_{16}\cdot 5\text{H}_2\text{O}$ nanobelts and nanorings. (c) HRTEM image of a typical $(\text{NH}_4)_2\text{V}_6\text{O}_{16}\cdot 5\text{H}_2\text{O}$ nanobelt. Left inset: the low-magnification TEM image of the nanobelts. Right inset: the SEAD pattern.

The morphology of the sample was checked by scanning electron microscopy (SEM). Figure S1 shows a typical panoramic FE-SEM image of the $(\text{NH}_4)_2\text{V}_6\text{O}_{16}$ product, where the dominant components are nanobelts with a uniform size distribution, with a little amount of nanoring structures. The nanobelts have a typical length of up to 100 μm , a width of about 100–200 nm, and a thickness of about 20–60 nm. Self-coiling of the polar nanobelts is evident (see the white circle in Figure S1), and the nanoring diameter is in the range of just below 1.0 μm to 5.0 μm . All the $\text{Na}_2\text{V}_6\text{O}_{16}$ nanorings have a perfect circular shape with very smooth and flat surfaces in the two typical forms of the perfect ring and the tape-like structure (in Figure S1). The more complex loop-like ring structures are also shown in the left of Figure S1, where the diameter of the microtube-like loop varies along the whole tube. Figure S1 c shows the HRTEM images and SAED patterns of the individual $(\text{NH}_4)_2\text{V}_6\text{O}_{16}\cdot 5\text{H}_2\text{O}$ nanobelts. The interplanar distances of 0.34 nm and 0.624 nm match well with the d_{110} and d_{200} spacings, respectively, of the monoclinic $(\text{NH}_4)_2\text{V}_6\text{O}_{16}\cdot 5\text{H}_2\text{O}$ nanobelt which is a single crystalline with the growth direction with [010] direction.

S2. $\text{K}_2\text{V}_6\text{O}_{16}\cdot 5\text{H}_2\text{O}$ nanobelts

Synthesis of $\text{K}_2\text{V}_6\text{O}_{16}\cdot 5\text{H}_2\text{O}$ nanobelts: $\text{K}_2\text{V}_6\text{O}_{16}\cdot 5\text{H}_2\text{O}$ nanobelts were synthesized in a similar hydrothermal process as $\text{Na}_2\text{V}_6\text{O}_{16}\cdot 3\text{H}_2\text{O}$ nanorings and nanoloops. The dosage of the corresponding material was the same. In a typical process, 2 mmol K_3VO_4 and 0.5 mmol K_2CO_3 powders were dissolved into 30 ml distilled water and strongly stirred for several minutes. Then 2 ml 30% hydrogen peroxide (H_2O_2) was added into the above suspension. After gently stirring at room temperature for 1 minute, the all solution was orange V(V) diperoxo aqueous solution with a pH of about 9.0, adjust the pH of the whole solution about 2.0 with 2 M HCl. At last the solution was transferred to a Teflon-lined stainless steel autoclave with a capacity of 42 ml, and the autoclave was sealed and maintained at 200 °C for 24 h. The reaction system was then allowed to cool to room temperature. The final product was collected by centrifugation, washed with deionized water and ethanol three times respectively to remove any possible ionic remnants, then dried in vacuum at 50 °C for 5 h.

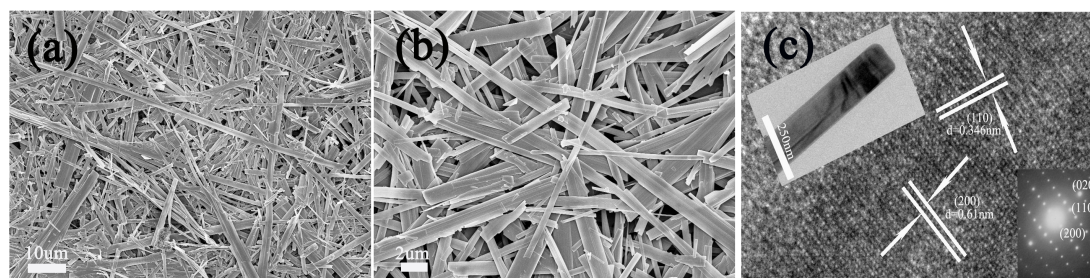


Figure S2. (a) Low- and (b) high-magnification FESEM images of the as-prepared $K_2V_6O_{16} \cdot 5H_2O$ nanobelts, (c) HRTEM image of a typical $K_2V_6O_{16} \cdot 5H_2O$ nanobelt. Left inset: the low-magnification TEM image of the nanobelts. Right inset: the SAED pattern.

The morphology of the sample was checked by scanning electron microscopy (SEM). Figure S2 shows a typical panoramic FE-SEM image of the $K_2V_6O_{16} \cdot 5H_2O$ product, where the components are nanobelts with a uniform size distribution. The nanobelts with very smooth and flat surfaces have a typical length of up to 100 μm , a width of about 400 nm – 1 μm , and a thickness of about 100 nm. Figure S2 c shows the HRTEM images and SAED patterns of the individual $K_2V_6O_{16} \cdot 5H_2O$ nanobelts. The interplanar distances of 0.346 nm and 0.610 nm match well with the d_{110} and d_{200} spacings, respectively, of the monoclinic $K_2V_6O_{16} \cdot 5H_2O$ nanobelt which is a single crystalline with the growth direction with [100] direction.

S3. The bandgap study of $Na_2V_6O_{16} \cdot 3H_2O$

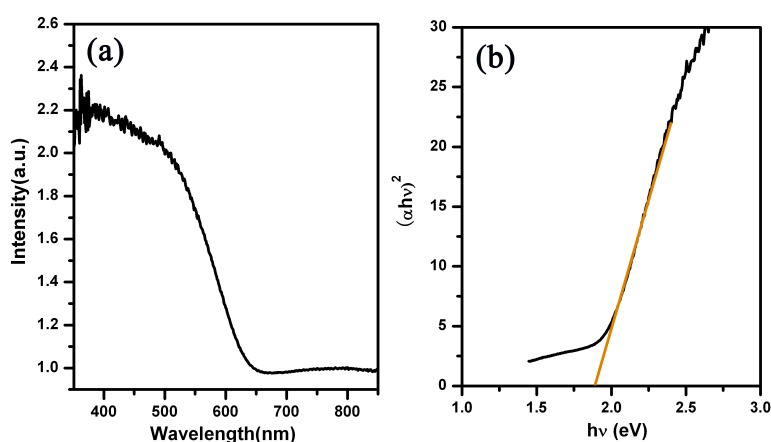


Figure S3. (a) UV-Vis spectrum of synthetic $Na_2V_6O_{16} \cdot 3H_2O$. (b) The UV-Vis Spectrum obtained by using the energy as abscissa of synthetic $Na_2V_6O_{16} \cdot 3H_2O$.

For a crystalline semiconductor, the optical absorption near the band follows the equation:

$$\alpha h\nu = A(h\nu - E_g)^{n/2}$$

Where α , ν , E_g , and A are absorption coefficient, light frequency, band gap, and a constant, respectively. Among them, n decides the kinds of direct-gap ($n = 1$) and indirect gap ($n = 4$) semiconductor in a materials. In this case, if the $n=4$ (indirect gap) is considered, the bandgap value is unacceptable due to the negative value; When $n=1$, the accepted bandgap value of 1.9 eV was obtained as shown in Figure 6b. Therefore, based on the careful analysis of UV-vis experimental results, the $Na_2V_6O_{16} \cdot 3H_2O$ is a direct-gap semiconductor with a bandgap of 1.9 eV.

S4. The I-V curve of $Na_2V_6O_{16} \cdot 3H_2O$ at 300K

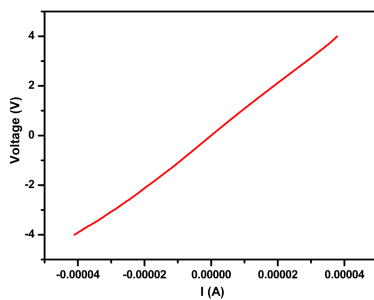


Figure S4. The I-V curve of $\text{Na}_2\text{V}_6\text{O}_{16}\cdot 3\text{H}_2\text{O}$ at 300 K.

The I-V curve of $\text{Na}_2\text{V}_6\text{O}_{16}\cdot 3\text{H}_2\text{O}$ at 300 K. is showed in Figure S4, and the average resistance is $1.06\text{E}+5 \Omega$.

S5. The magnified low-magnification FESEM images of the $\text{Na}_2\text{V}_6\text{O}_{16}\cdot 3\text{H}_2\text{O}$ sample and nanoloops

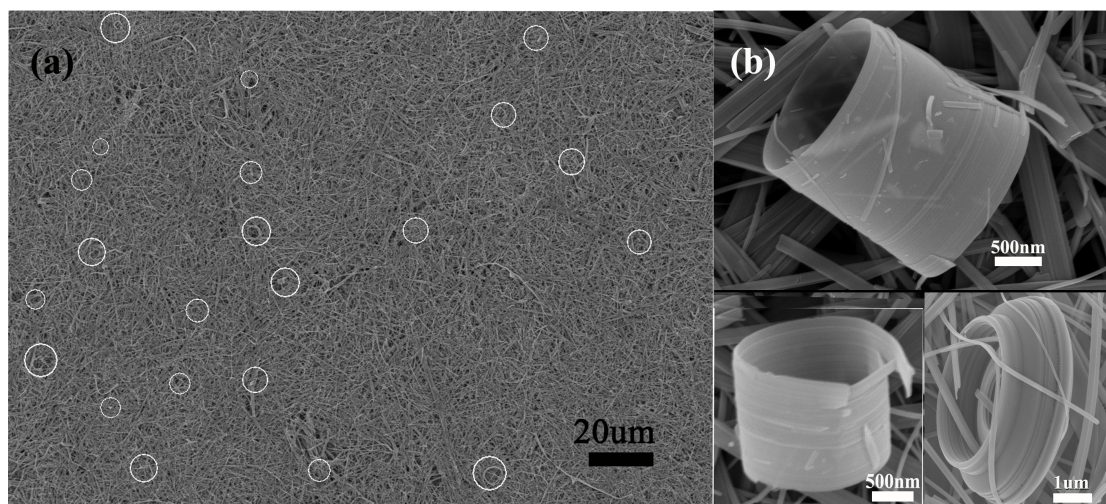


Figure S5. The magnified low-magnification FESEM images of the $\text{Na}_2\text{V}_6\text{O}_{16}\cdot 3\text{H}_2\text{O}$ sample (a) and nanoloops (b).